Int. J. Therm. Sci. (2000) 39, 404–413

S1290-0729(00)00218-0/FLA

Local convective heat exchanges from a rotor facing a stator

Souad Harmand [a]*, Barbara Watel [b], Bernard Desmet [a]

[a] *Laboratoire de Mécanique et Energétique, Université de Valenciennes et du Hainaut-Cambrésis, Le Mont Houy, 59313 Valenciennes cedex 9, France*

[b] *Université Joseph Fourier–Grenoble 1, Département Génie Thermique et Energie, 39-41, Boulevard Gambetta, 38000 Grenoble, France*

(Received 24 March 1999, accepted 1 September 1999)

Abstract — The local convective heat transfer from a rotor with a 310 mm outer radius is studied experimentally at a distance of 3 mm from a coaxial crown-shaped stator with a 176 mm inner radius and a 284 mm outer radius. The experimental technique is based on the use of a thermally thick rotor heated from behind by infrared radiation. The local heat flux distribution from the rotor surface is identified by resolving the Laplace equation by finite difference method using the experimental temperature distribution as boundary conditions. The tests are carried out with the single rotor and the stator/rotor system for local rotational Reynolds numbers ranging from $2.0{\cdot}10^4$ to $1.47{\cdot}10^6$ and thus sweeping across the laminar, transition and turbulent flow regimes. The local and mean Nusselt numbers for the single disc are compared with those obtained experimentally for the stator/rotor system. The flow structure in the space between the rotor and the stator is analysed by Particule Image Velocimetry. © 2000 Éditions scientifiques et médicales Elsevier SAS

heat transfer / local heat flux / forced convection / stator / rotor

Nomenclature

c	constant	
e	thickness of the PES disc	m
G	$= s/R_{\text{ext}}$, gap ratio	
h	local heat transfer coefficient	$\text{W}{\cdot}\text{m}^{-2}\text{K}^{-1}$
$\bar{h}$	mean heat transfer coefficient	$\text{W}{\cdot}\text{m}^{-2}\text{K}^{-1}$
J	radiosity	$\text{W}{\cdot}\text{m}^{-2}$
n	constant	
Nu	$= hr/\lambda$, local Nusselt number on the rotor facing the stator	
$\overline{Nu}$	$= \bar{h}R_2/\lambda$, mean Nusselt number on the rotor facing the stator	
Nu_∞	local Nusselt number on the isolated rotor	
$\overline{Nu}_\infty$	mean Nusselt number on the isolated rotor	
r	radial position on the rotor	m
r^*	$= (r - R_1)/(R_2 - R_1)$, dimensionless radius	
R_1, R_2	internal and external study zone radius	m
R_{1s}, R_{2s}	internal and external stator radius . .	m
R_{ext}	rotor external radius	m
Re	$= \omega R_2^2/\nu$, peripheral Reynolds number	
Re^*	$= \omega r^2/\nu$, local Reynolds number	
s	spacing between the rotor and the stator	m
T	temperature	K
u_ϕ	tangential velocity component	$\text{m}{\cdot}\text{s}^{-1}$
$u_{\phi,\text{c}}$	tangential velocity component in the gap mid-plane	$\text{m}{\cdot}\text{s}^{-1}$
v_r	radial velocity component	$\text{m}{\cdot}\text{s}^{-1}$
z	axial coordinate in the disc	m
z'	axial coordinate in the air-gap	m

Greek symbols

ε	emissivity	
λ	thermal conductivity	$\text{W}{\cdot}\text{m}^{-1}{\cdot}\text{K}^{-1}$
ν	kinematic viscosity	$\text{m}^2{\cdot}\text{s}^{-1}$
τ	transmission coefficient	
φ_{cd}	conductive heat flux	$\text{W}{\cdot}\text{m}^{-2}$
φ_{cv}	convective heat flux	$\text{W}{\cdot}\text{m}^{-2}$
φ_r	radiative heat flux	$\text{W}{\cdot}\text{m}^{-2}$
ω	rotational speed	$\text{rad}{\cdot}\text{s}^{-1}$

* Correspondence and reprints.
Souad.Harmand@univ-valenciennes.fr

Subscripts

a air
r rotor
s stator
∞ value far from rotor

1. INTRODUCTION

This study aims to analyse the local convective heat transfer from the plane surface of a rotating disc of outer radius R_{ext}, facing an annular stator between the radii R_{1s} and R_{2s}, at distance s from the disc (*figure 1*).

The convective heat transfer from a disc rotating in rest air has been studied by different autors. In the case of a disc rotating in free air, with a power-law temperature profile $T(r) = T_\infty + cr^n$, Dorfman [1] proposes correlations giving the local Nusselt number:

- $Nu_\infty = 0.221\sqrt{n+2}(Re^*)^{0.5}$ for the laminar flow ($Re^* \leq 1.82{\cdot}10^5$),
- $Nu_\infty = 0.0169(n+2.6)^{0.2}\ (Re^*)^{0.8}$ for the turbulent flow ($Re^* \leq 2.82{\cdot}10^5$).

In the case of rotor/stator systems, Owen [2] and Kreith [3] distinguish four flow regimes depending on the rotational speed and gap between the disc and the stator. Regime I corresponds to laminar boundary layers on the two parallel surfaces which touch and give rise to the low gap ratio $G = s/R_{ext}$. Regime II is obtained for high G values, when there are two laminar boundary layers, one on the rotor and another on the stator, separated by a core of fluid rotating at approximatively 0.4ω. Regimes III and IV are respectively equivalent to regimes I and II but for turbulent boundary layers. In the case of a rotating disc with a quadratic surface temperature profile $T(r) = T_\infty + cr^2$, parallel to a stationary isothermal full disc at T_∞, Dorfman [1], Owen [2] and Kreith [3] showed that for regime I, $\overline{Nu}$ is independent of Re ($\overline{Nu} = G^{-1}$), and that for regime III, $\overline{Nu}$ depends on $Re^{0.75}$ ($\overline{Nu} = 9.8{\cdot}10^{-3}G^{-1/4}Re^{0.75}$). For regime II a radial outflow of fluid which is carried from the core is observed close to the rotor. On the stator, there is a radial inflow of fluid and mass transfer from the boundary layer to the core (Batchelor [4]). For intermediate gaps, Owen [5] clearly shows that the rotating core of fluid reduces shear stress on the rotor and the value of $\overline{Nu}$ therefore falls below that of the free disc. For regimes II and IV (high G values), the mean Nusselt number is a G increasing function. Owen [5] shows the existence of a ratio G for which the mean Nusselt number is a minimum which corresponds to the transition between regime III and regime IV. Several authors have suggested estimating the G value above which the Nusselt number on the rotor is not affected by the presence of the stator with the following equation:

$$G_{lim} = 1.05Re^{-0.2} \quad (1)$$

Owen [2] studied the influence of a radial outflow of air to the rotor/stator. He classified the flow into four regimes as in the case of a full stator for the air-cooled rotating disc.

In the present experimental analysis of the rotor/stator system, the gap ratio is $G = 0.01$ and the peripheral Reynolds number Re varies from $5.86{\cdot}10^4$ to $1.47{\cdot}10^6$. The experimental method used to determine the local heat transfer coefficients is based on the determination by infrared thermography of the surface temperatures of a low conductive coating on the rotating disc. This coating is designed so that it behaves as a thermally thick wall. For each rotational speed, the local and mean Nusselt numbers are compared with those obtained for the single rotor. Particle Image Velocimetry (PIV) analyses the flow structure in the space between the rotor and the stator.

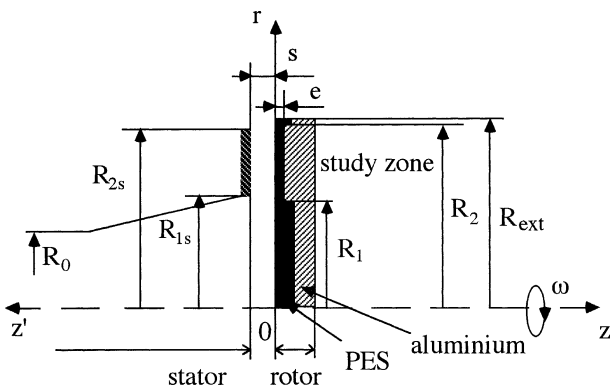

Figure 1. Diagram of rotor/stator system.

2. DESCRIPTION OF TESTS

2.1. Experimental set-up

A thick aluminium disc and a polyethersulfone (PES) layer with a thickness $e = 2$ mm in the study zone ($R_1 < r < R_2$) constitute the rotor [6]. The geometrical parameters of the test bench (*figure 1*) are: $R_1 = 170$ mm, $R_2 = 290$ mm, $R_{1s} = 176$ mm, $R_{2s} = 284$ mm, $R_{ext} = 310$ mm and $s = 3$ mm. The PES part of thermal conductivity $\lambda_r = 0.36\ W{\cdot}m^{-1}{\cdot}K^{-1}$, facing the sta-

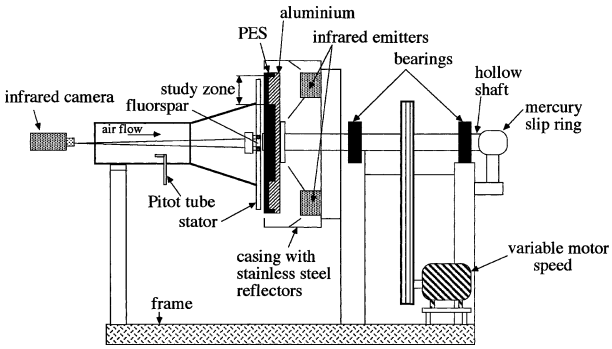

Figure 2. Experimental set-up.

tor (*figure 2)* is stuck on the aluminium disc, the rear face of which is subjected to infrared radiation. As the values of the PES thermal conductivity and PES thickness are low, the variations in the heat transfer coefficients on the PES surface are translated into temperature variations on this surface. The high values of the aluminium conductivity and the disc thickness allow one to homogenize the temperature at the aluminium/PES interface. The rotor rotational speed varies from 100 to 2 400 rev·min^{-1}. The steel stator is equipped with a fluorspar window so that the temperature on the rotor can be identified by infrared thermography. The temperatures at the PES/aluminium interface are measured by two thermocouples bound to the acquisition system with a mercury ring rotating collector. The absolute error on the temperature at the PES/aluminium interface is estimated at $\Delta T = \pm 0.3$ K. The temperatures recorded by these thermocouples, ranging from 50 to 150 °C, have at most 0.4 K difference for all the tests. The air reference temperature T_∞ is measured by a thermocouple in the test room, far from the disc. The absolute error on T_∞ is estimated at $\Delta T_\infty = \pm 0.3$ K. The stator temperature is measured by two K type thermocouples located at two different radii on its surface parallel to the rotor. The absolute error on the stator temperature, ranging from 40 to 50 °C, is estimated at $\Delta T = \pm 0.4$ K. For all the tests, the stator temperature is quasi-uniform and the stator is considered isothermal. Temperature difference between the stator and the air is around 15 K.

The rotor surface temperature is obtained from the thermal level measured by a short wave infrared camera which is used in line scanning mode at a 3 472 Hz frequency. The line scanning is achieved along a radius of the rotor study crown through a fluorspar window (*figure 2*). The transmission coefficient of the fluorspar, obtained by calibration, is $\tau_f = 0.95 \pm 0.03$ in the camera wavelength range ($2\ \mu m < \lambda < 5\ \mu m$). To favour the rotor thermal emission when compared with the reflected parasitic radiation flows, the rotor surface is covered with black paint. Calibration determines the rotor emissivity $\varepsilon_r = 0.93 \pm 0.02$ and the stator emissivity $\varepsilon_s = 0.65 \pm 0.03$. In order to take the parasitic heat fluxes reflected by the rotor surface into account, its radiosity is determined from the radiative exchange balance between the disc and the stator. The error estimate on the rotor temperature T gives $\Delta T = 0.90$ K for our temperature range $50 < T < 150$ K.

The mean flow fields are obtained by the Particle Image Velocimetry (PIV) in the mid-plane between rotor and stator. The air velocity in the pulsed laser sheet is obtained by determining particle displacement over time using a double-pulsed laser technique. The laser light sheet illuminates the mid-plane in the flow and the position of particles in that plane are recorded by the camera. After a short time interval, a second laser pulse illuminates the same plane, creating a second image of the particles. The velocity vectors in the plane are obtained by using a cross-correlation between the two images.

2.2. Heat flux identification

The numerical solution of the energy equation for a stationary regime allows to give the local heat transfer coefficient at a given position on a radius of the rotor study zone. Considering the model design and flow conditions, the temperature distribution inside the rotor is supposed to be axisymmetrical. In this case, the energy equation in the rotor in PES is written:

$$\frac{\partial^2 T}{\partial r^2} + \frac{1}{r}\frac{\partial T}{\partial r} + \frac{\partial^2 T}{\partial z^2} = 0 \qquad (2)$$

The boundary conditions known in the study are: for $z = 0$, $T(r, 0)$ is given by the camera, and for $z = e$, $T(r, e)$ is given by the thermocouples. For the boundary conditions on the surfaces ($r = R_1$; z) and ($r = R_2$; z), the influence of a heat flux equal to zero and this of a linear temperature variation calculated from the surface temperature measurements has been studied. Thus, it has been deduced that the influence of these two different boundary conditions on the results is limited to very small peripheral zones (near radii R_1 and R_2). In order to solve these equations, a finite difference method has been used. The local wall heat flux on the rotor surface submitted to the cooling can be calculated by:

$$\varphi_{cd} = \lambda_r \left(\frac{\partial T}{\partial z}\right)_{z=0} = \varphi_{cv} + \varphi_r \qquad (3)$$

where $\varphi_{cv} = h(T_0(r) - T_\infty)$ represents the convective heat flux from the rotor to the air, and

$$\varphi_r = \frac{\varepsilon_r}{1-\varepsilon_r}\left(\sigma T_0^4(r) - J_r\right)$$

the radiative heat flux from the rotor towards its environment. The radiosity J_r of the rotor is estimated by considering an enclosure constituted by the rotor surface of emissivity ε_r, the stator surface of emissivity ε_s, the stator central opening and the peripheral crown between the rotor and the stator that behave like black surfaces at T_∞. The local and mean Nusselt numbers are then deduced:

$$Nu = \left[\frac{\lambda_r(\partial T/\partial z)_{z=0} - [\varepsilon_r/(1-\varepsilon_r)](\sigma T_0^4(r) - J_r)}{T_0(r) - T_\infty}\right]\frac{r}{\lambda_a} \tag{4}$$

$$\overline{Nu} = \frac{\overline{h}R_2}{\lambda_a} = \frac{2R_2}{R_2^2 - R_1^2}\frac{1}{\overline{T - T_\infty}}\int_{R_1}^{R_2} Nu\,(T - T_\infty)\,\mathrm{d}r \tag{5}$$

3. RESULTS AND ANALYSIS

3.1. Structure of the flow

Tests were carried out for peripheral Reynolds numbers between $5.86{\cdot}10^4$ and $1.47{\cdot}10^6$. For this Reynolds numbers range, the G_{lim} value defined by (1) varies between 0.05 and 0.12. As in the experimental set-up, the G value is equal to 0.01, so one can expect to have an interaction of the boundary layers built up on the disc and the stator, without the building up of a rotating core, whatever *Re* is. In these test conditions, the flow remains next to the Couette-type flow for which the viscous region fills the whole space between the disc and the stator.

The study of the flow field in the mid-plane between the rotor and the stator is carried out by PIV, for rotational speeds between 200 and 2 400 rev·min^{-1}. A positioning system, constituted by a rotary table with two degrees of freedom and a micrometric screw for the translation allows to position the laser sheet in the midplane between the rotor and the stator with an uncertainty equal to ± 0.2 mm. The laser sheet thickness is equal to 0.5 mm.The flow field is only obtained in the air-gap zone, corresponding to $R_1 \leq r \leq R_2$ (*figure 3*). When $r < R_1$, that is in front of the stator opening, the flow near the disc is expected to be similar to that obtained near a single disc and there is a zone of aspiration in front of the disc where the axial velocity is non-negligible. On the other hand, for $r > R_1$, the disc and the stator impose predominant radial and tangential directions. The stator opening being much larger than the air-gap, the fluid pumped by the rotor is supplied at the stator opening and all the flow is outward in the air-gap. The fluid then flows from the stator opening to the disc periphery. Moreover, the measurements of the air flow rate q_v due to the fluid pumped by the rotor and supplied at the stator opening have been carried out for different disc rotational speeds (*figure 4*). The velocity of the air aspirated into the inlet pipe is measured by a Pitot tube connected to a micro manometer (*figure 2*) and the relative error on the velocity is estimated at $\pm 5\,\%$. The aspirated air flow is determined then using the air velocity profile measured in the pipe. The pumped in air flow rate varies from 0.010 m$^3{\cdot}$s^{-1} to 0.045 m$^3{\cdot}$s^{-1} with the increase in the rotational speed from 300 to 2 300 rev·min^{-1}, which shows the importance of the fluid pumping due to the disc rotation. Contrary to the configuration of the disc facing a plane surface, as studied by Kreith [3], in this case there is a circular opening at the stator centre and the air-gap freely emerges into the atmosphere. It favours an outward flow of fluid in the air-gap, as can be seen in *figure 5a*, whatever the rotational speed. The velocity radial component tends to decrease with the increase in the radius. The evolution of the velocity radial component obtained by PIV is shown in *figure 5a* for a test at $\omega = 300$ rev·min^{-1}. The air mass flow rate being conserved from the entrance to the exit of the air-gap, the decrease in the radial velocity as a function of the radius is explained by the increase in the passage section of the fluid. All the flow being outward in the air-gap, the conservation of the mass flow rate is therefore expressed by the equation:

$$R_1\int_0^s v_r(r = R_1, z')\,\mathrm{d}z' = r\int_0^s v_r(r, z')\,\mathrm{d}z' = r\,v_{rm}$$

The radial velocity averaged along z', v_{rm}, also varies according to a hyperbolic law in $1/r$: $v_{rm} = q_v/(2\pi rs)$. The radial evolution of v_{rm} is plotted in *figure 5a*. The discrepancies observed can be explained, on the one hand, by the velocity axial distribution in the air-gap that leads to a velocity in the mid-plane which can be different from the average velocity and, on the other hand, by the error on the location of the laser sheet between the rotor and the stator. Indeed, the Reynolds number of the source flow in the air-gap is around 200, which is at the origin of a relatively flat velocity profile in the air-gap at $R_1 = 0.17$ m, whereas the velocity profile near the

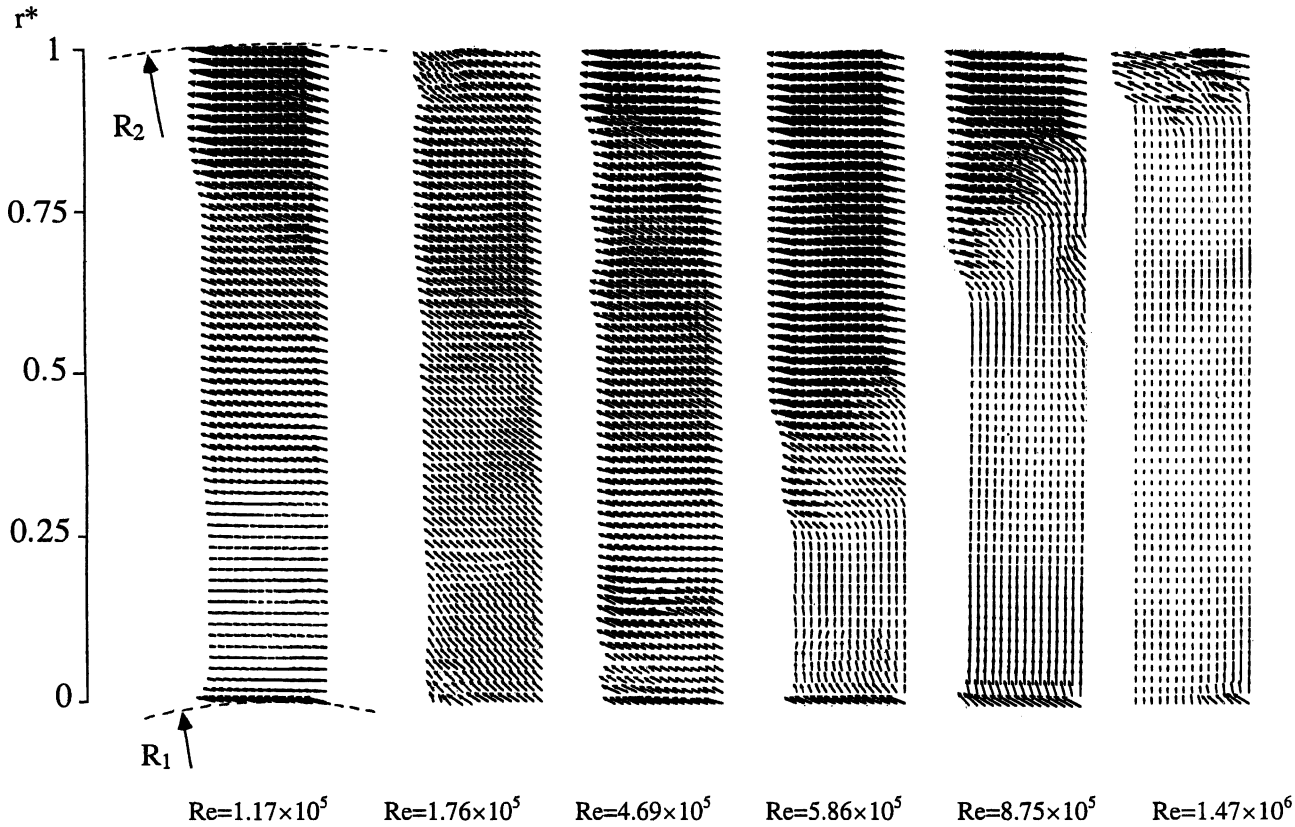

Figure 3. Flow field in the mid-plane between the disc and the stator obtained by PIV for various *Re*.

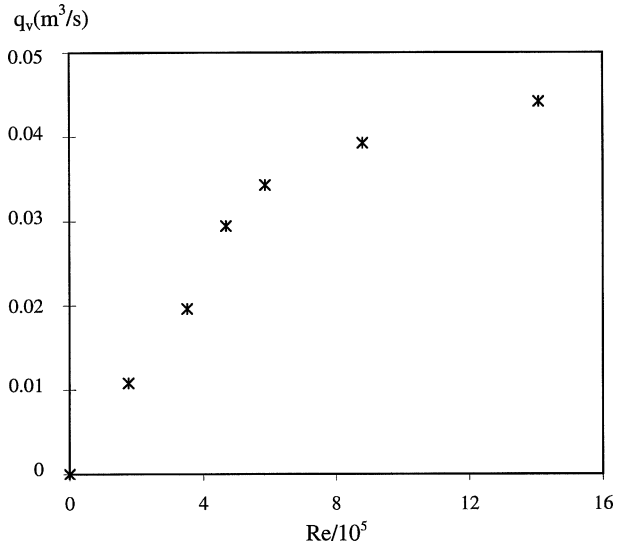

Figure 4. Flow-rate variations as a function of the peripheral Reynolds number.

exit at $r = 0.290$ m is more parabolic. At this radius, the maximum velocity is not obtained in the mid-plane and an error on the position of the laser sheet can explain the differences observed in *figure 5a*.

Moreover, an overall increase in the velocity tangential component as a function of the radius can be seen in *figure 3*. *Figure 5b* gives the evolution of the tangential component $u_{\phi,c}$ as a function of the radius for $\omega = 300$ rev·min^{-1}. Indeed, the thickness of the boundary layers and the interaction of the boundary layers built up on the disc and the stator increase in the flow direction, i.e. towards the disc periphery. This, therefore, favours a flow in the tangential direction at the high radii. Moreover, Owen [2] showed that for a Couette-type flow for which the viscous region fills the whole space between the disc and the stator, the tangential component of the flow velocity for a given z' in the air-gap linearly increases as a function of the radius. The differences in relation to the linear law are particularly significant in the zone of the flow establishment at the air-gap entrance.

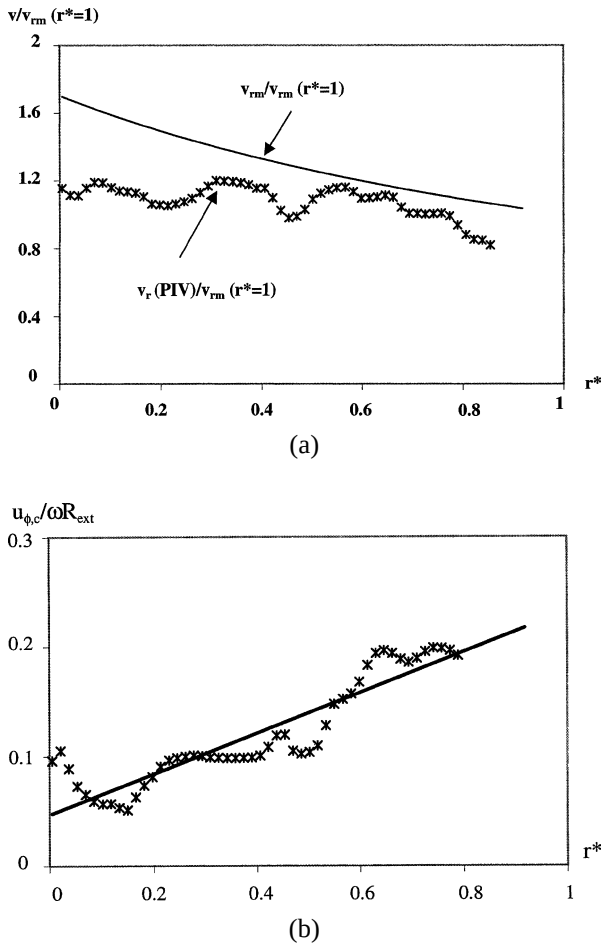

Figure 5. (a) Evolution of the mean radial velocity and the radial component mesured by PIV. (b) Variation of the tangential velocity as a function of dimensionless radius.

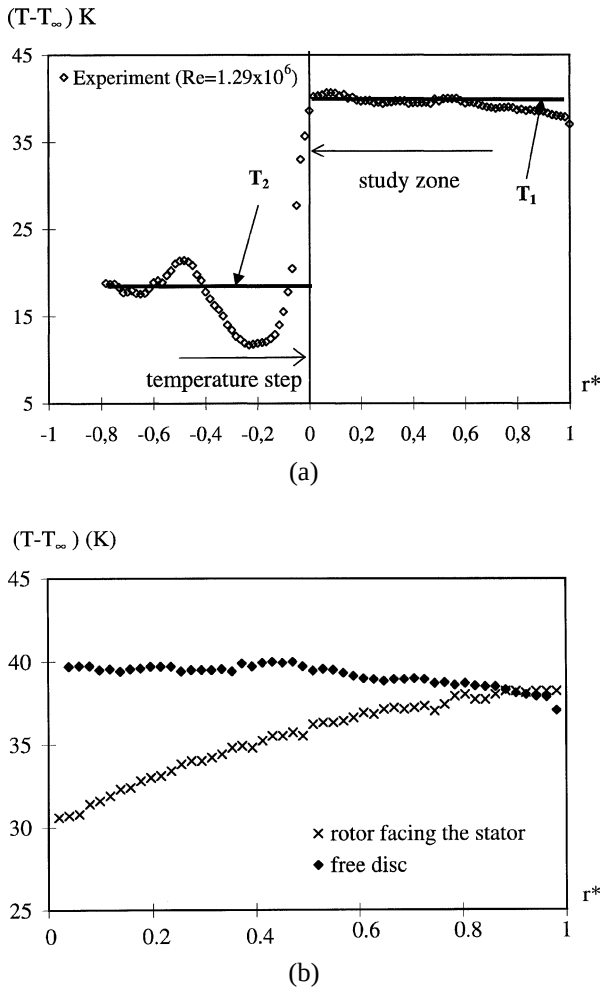

Figure 6. (a) Temperature profiles of the surface of the disc $Re = 1.29{\cdot}10^6$ ($0 < r^* < 1$ and $0.170 < r < 0.290$ m). (b) Temperature profile of the surface of the free disc ($-1 < r^* < 1$ and $0 < r < 0.290$ m).

The decrease in the radial velocity with the increase in the radius due to the mass flow rate conservation and the increase in the tangential velocity as a function of the radius therefore explain why, at the high radii, the fluid movement is made mainly in the tangential direction.

The comparison of the flow fields for the different rotational speeds shows that the radius above which the velocity tangential component becomes preponderant, when compared with the radial component, increases with the rotational speed. At the low rotational speeds, the inertial terms, and particularly the term relative to the centrifugal effects, are negligible in the space between the rotor and the stator when compared with the tangential component of the shear stress, favouring therefore a flow in the tangential direction. Furthermore, as the boundary layer thickness on the disc increases as *Re* decreases, the radial circulation of the fluid is more difficult than at high velocities because of the more significant viscosity forces. With the increase in *Re*, the fluid radial circulation is easier initially at the small radii where the boundary layer is not as thick.

3.2. Results of the tests on the convective heat transfer

3.2.1. Temperature profiles

The representation of the temperature difference $(T - T_\infty)$ as a function of dimensionless radius $r^* = (r - R_1)/(R_2 - R_1)$ shows (*figure 6a*) that there is a weak temperature variation in the study zone and a big drop in

temperature at dimensionless radius $r^* = 0$ corresponding to the beginning of the study zone. The temperature difference between 15 and 30 K for all these tests is due to the increase in the PES thickness in this zone. In a simplified way, the radial temperature profile on the disc surface can be represented by the following law: for $r < R_1,\ T = T_1$ and for $r \geq R_1,\ T = T_2$. The dimensional analysis [6] shows that the local Nusselt number on the rotor surface with a temperature step is expressed as a function of

$$\left(Pr,\ Re^*,\ \frac{T_2 - T_1}{T_2 - T_\infty},\ \frac{T_2 - T_s}{T_2 - T_\infty}\right)$$

This relation shows that the local heat transfer coefficient in the study zone ($R_1 \leq r \leq R_2$) depends on the temperature step ($T_2 - T_1$). It is, therefore, preferable to compare experimental values of the local heat transfer coefficient for the disc without the stator with the correlations in literature which best express this temperature evolution along the radius. The only laws found in the bibliography dealing with a high radial temperature gradient on the disc correspond, therefore, to power-law temperature profiles and in particular to a quadratic temperature distribution. Furthermore, Dorfman [1] showed that it is essential to take the influence of a radial temperature gradient on the disc into account when evaluating the local heat transfer coefficient. That is why the experimental temperature evolution on the disc surface is interpolated by a power-law of the form $T = T_\infty + cr^n$ where exponent n is a function of the disc rotational speed. The experimental temperature profiles on the PES surface in contact with the air are plotted in *figure 6b* for peripheral Reynolds number $Re = 1.29{\cdot}10^6$. These profiles are only given in the study zone $0 < r^* < 1$ for the case of the single disc and the stator/rotor system. One notices that on the single disc the temperature in the study zone is quasi-constant between $r^* = 0$ and $r^* = 0.53$ and then slowly decreases until $r^* = 1$. This decrease towards the disc periphery is due to an increase in the convective transfer as a function of the radius. On the rotor surface facing the stator, the temperature variation in the study zone is higher than on the single disc surface and the temperature is a radius increasing function contrary to the single disc. These trends are observed for each rotational speed.

The relative importance of the convective and radiative losses is analyzed by calculating ratio φ_r/φ_{cv} (cf. (3)). In the case of the rotor facing the stator, this ratio accepts a maximum equal to 15 % for the test at $Re = 5.86{\cdot}10^4$ and a minimum equal to 3 % for $Re = 1.47{\cdot}10^6$. In the case of the single rotor, φ_r/φ_{cv} is equal to 50 % for the test at $Re = 5.86{\cdot}10^4$ and admits a minimum of 6 % for $Re = 1.47{\cdot}10^6$. At the low Reynolds numbers, the radiative losses represent a non-negligible part of the whole losses and must be taken into account in the calculation of the convective exchanges.

3.2.2. Local Nusselt number

The definitions of the local and mean Nusselt numbers given by equations (4) and (5) are adopted. In *figure 7*, the local Nusselt numbers are plotted as a function of the dimensionless radius r^* for different peripheral rotational Reynolds numbers *Re*. The results relative to the single disc without stator and Dorfman's results on the single rotating disc are also plotted. *Figure 7a* represents the experimental results for $Re = 1.17{\cdot}10^5$ for which the flow is laminar on the single disc. In the case of the free disc, the Nusselt number is in good correlation with Dorfman's results with, however, a slight increase next to the temperature step. The local convective exchange is uniform on the disc study zone except near the temperature step. In the case of the rotor facing the stator, the Nusselt number is practically constant on all the crown surface which corresponds to a non-uniform convective exchange on the rotor: it is higher at the inner radius of the rotor study zone than at the outer radius. The experimental results for $Re = 1.76{\cdot}10^5$ and $Re = 2.35{\cdot}10^5$ are plotted in *figures 7b* and *c*. In the case of the free disc, this Reynolds number range corresponds to the laminar/turbulent transition. For $Re = 1.76{\cdot}10^5$, the experimental results on the free disc are higher than those of Dorfman for a laminar flow and closer to the author's results obtained for a turbulent flow. In the case of the rotor facing the stator, the Nusselt number remains approximately constant on all the crown surface and the relative gap in comparison with an average value is 6 %. For $Re = 2.35{\cdot}10^5$, in the case of the free disc, the experimental results are higher than those given by Dorfman's correlation for a turbulent flow. A significant increase in the convective exchange is noticed at this Reynolds number which could correspond to a laminar/turbulent transition over the disc. In the case of the rotor facing the stator, the Nusselt number remains constant in the study zone and the heat transfer coefficient is higher for the lowest radii and weaker near the periphery. In *figures 7d* and *e* corresponding to $Re = 3.52{\cdot}10^5$ and $Re = 4.69{\cdot}10^5$, the flow is completely turbulent over the free disc. The experimental results are in good correlation with those of Dorfman except near the temperature step where a slight increase in the Nusselt number is observed for the experimental configuration. The convective heat transfer from the free disc is higher at the high radii. For the rotor facing the stator, the Nusselt number remains constant and the

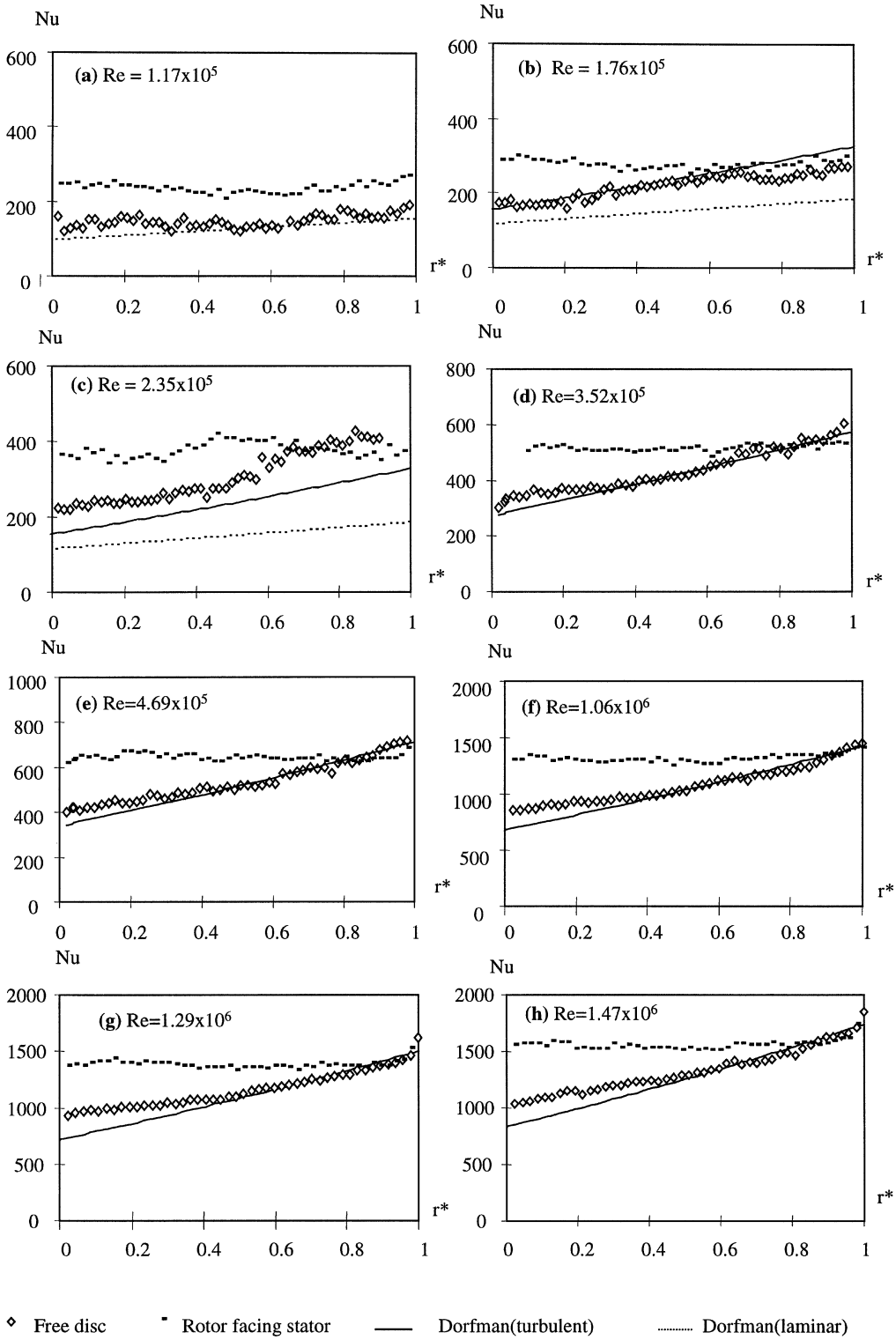

Figure 7. Local Nusselt number as a function of the dimensionless radius for different *Re*.

convective exchanges are a radius decreasing function whereas for the free disc they are a radius increasing function. In *figures 7f, g* and *h*, our results relative to Reynolds numbers $Re = 1.06{\cdot}10^6$, $Re = 1.29{\cdot}10^6$ and $Re = 1.47{\cdot}10^6$ are plotted. The previous comments about the evolution of the convective heat transfer in the study zone of the disc and the rotor facing the stator are confirmed.

According to our tests, the distribution of the local Nusselt number as a function of the radius in the rotor/stator configuration significantly differs from that obtained on the single disc. For the rotor/stator system, the local Nusselt number remains almost independent from the radius. Some authors, such as Patra [7] and Soong [8], explain the decrease in the convective exchanges as a function of the radius by the decrease in the radial velocity as a function of the radius, as was noticed previously with the analysis of the PIV results. This analysis is, however, not sufficient because it does not take the influence of the fluid tangential velocity into account. Actually, the norm of the fluid relative velocity in relation to the disc $v_{\text{rel}} = ((\omega r - u_\phi)^2 + v_r^2)^{1/2}$ is probably more representative when identifying the influence of the flow velocity on the convective transfer. Velocity v_{rel} computed in the mid-plane between the rotor and the stator is plotted in *figure 8* as a function of the radius for the test at $\omega = 300$ rev·min^{-1}. As the velocity v_{rel} increases as a function of the radius, the evolution of the flow velocity in the mid-plane does not allow one to interpret the thermal results. The radial evolution of the thermal boundary layer thickness on the disc can however explain our thermal results. Indeed, for the air-gap studied, the flow is outward and the fluid supplied by the stator opening is rejected towards the disc periphery. The fresh air supply comes through the stator opening. The fluid in the air-gap heats in the flow direction. This corresponds to an increase in the thermal boundary layer thickness because in the air-gap there is no fresh fluid supply on the rotor facing the stator, contrary to the case of the single disc. The air temperature was measured by thermocouples at the air-gap entrance (T_{ent}) and at the air-gap exit (T_{exit}). In particular, for the test at $\omega = 300$ rev·min^{-1}, the measurements are: $T_{\text{ent}} = 34\,^\circ$C and $T_{\text{exit}} = 40\,^\circ$C. These values confirm the fluid heating in the flow direction. The fluid temperature towards the periphery approaches that of the disc, causing the decrease in the convective heat transfer from the disc.

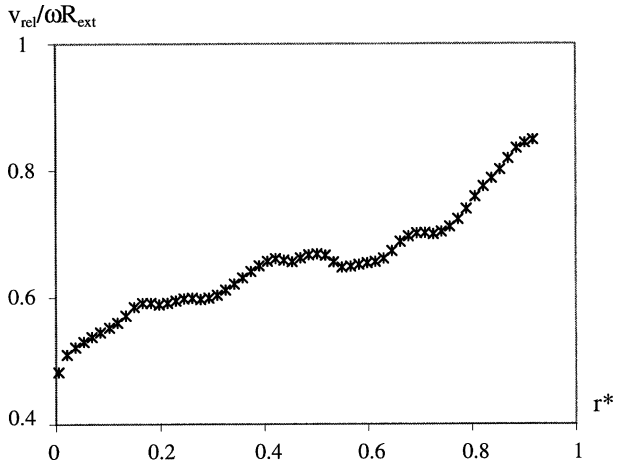

Figure 8. Variation of the relative velocity as function of the dimensionless radius.

3.2.3. Mean Nusselt number

The evolution of the mean Nusselt number in the study zone as a function of the peripheral Reynolds number is plotted in *figure 9*, for the free disc and the rotor/stator system. The mean Nusselt number $\overline{Nu}$ for the stator/rotor system is higher than Nusselt number $\overline{Nu}_\infty$ obtained on the single disc. It is deduced from the bibliography that ratio $\overline{Nu}/\overline{Nu}_\infty$ depends on the air-gap ratio G. According to Owen [5], for the very low G values (≤ 0.01), a Couette flow region extends from the rotor to the stator, causing large shear stresses which give rise to the Nusselt number values in excess of the free disc level. It is deduced from this study and from Owen's conclusions that, with our configuration, the regime of flow studied is close to the Couette flow. As the experimental results of Owen [5] show, the Nusselt number is a Reynolds number increasing function, within the range $8.0{\cdot}10^{-3} \leq G \leq 10^{-2}$. For our experimental results, the gradient of the representation $Nu = f(Re)$ for a logarithmic scale, decreases with the decrease in the Reynolds number

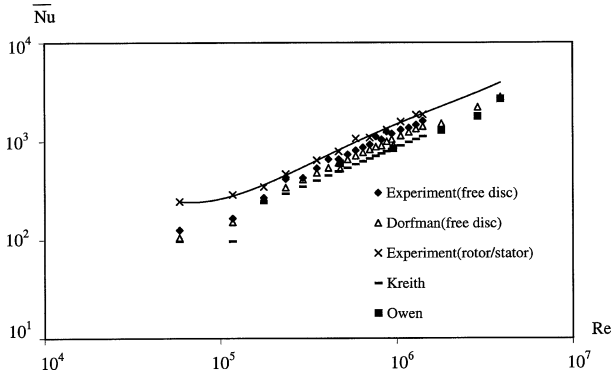

Figure 9. Mean Nusselt number as a function of peripheral Reynolds number *Re*.

(the *Re* power varies from 0.8 for high *Re* to 0.3 for weak *Re*). This can be explained by a change in the flow regime: the 0.8 gradient suggests a turbulent flow at high velocities. For a laminar Couette flow, the Nusselt number should be independent from the rotational speed. The 0.3 slope at the weak rotational speeds shows that the flow is located in a transient regime and for lower *Re*, $\overline{Nu}$ should accept a limit value. Moreover, in the Reynolds number range which corresponds to a turbulent flow over the disc, for both the rotor/stator system and the single disc, the Nusselt number is expressed as a 0.8 power law and ratio $\overline{Nu}/\overline{Nu}_\infty$ is equal to around 1.25.

On the other hand, for Reynolds numbers lower than $1.17 \cdot 10^5$ which correspond to a laminar flow over the disc, the relative discrepancies between the Nusselt number on the rotor and that on the single disc considerably increases. Whereas the Nusselt number on the single disc is expressed as a 0.5 power law, the Nusselt number on the rotor facing the stator is very close to an asymptotic value independent from the Reynolds number, corresponding to a Couette flow. The flow in the air-gap actually becomes more distant from the flow obtained next to the single disc with the decrease in the Reynolds number. However, with the increase in *Re*, the interaction of the boundary layers decreases (their thickness decreasing with the increase in *Re*) and the flow in the air-gap becomes closer to the flow obtained over the single disc.

The comparison of our experimental results for the rotor/stator system with those of Owen and Kreith shows significant differences between the $\overline{Nu}$ values. These differences are not surprising since there are significant differences between the configurations, in the geometry as well as in the thermal boundary conditions on the different surfaces. In Owen's [5] and Kreith's studies [3], the stator central opening is very small whereas it is larger in our study. The stator surface temperature is T_∞ in the study of these authors whereas in our tests the stator is heated. Temperature distribution on the disc is also different for our tests and for those of Owen [5] and Kreith [3].

4. CONCLUSION

The study of the flow structure in the mid-plane between the two discs by PIV shows that the presence of a large central opening in the stator causes the fluid to flow in and its mass flow rate increases with rotational speed. The flow at the central opening of the stator moves radially outwards and the increase in the passage section of the fluid between the two parallel surfaces as it gets nearer the periphery causes a decrease in the radial velocity. The PIV results show, however, that the fluid tangential velocity in the air-gap increases with the radius and that the flow is mainly in the tangential direction at the high radii. Moreover, the comparison of our experimental results for local convective exchanges from the rotor facing the stator in the study zone and the free disc give rise to the following conclusions: the local convective heat transfer decreases as a function of the radius on the rotor facing a crown-shaped stator and featuring a large central opening, contrary to the free disc. The fresh air supply is through the stator opening. The fluid in the air-gap heats in the flow direction. There is no fresh fluid supply to the rotor facing the stator, contrary to the single disc, and the fluid temperature approaches that of the disc, thereby causing the decrease in the convective heat transfer from the disc towards the periphery.

REFERENCES

[1] Dorfman L.A., Hydrodynamic Resistance and Heat Loss from Rotating Solids, transl. by Kemmer N., Oliver and Boyd, Edinburgh, London, 1963.

[2] Owen J.M., Rogers R.H., Flow and Heat Transfer in Rotating-Disc Systems, Vol. 1, Rotor–Stator Systems, Research Studies Press Ltd., 1989.

[3] Kreith F., Convection heat transfer in rotating system, Adv. Heat Tran. 5 (1968) 129–251.

[4] Batchelor G.K., Note on a class of solutions of the Navier–Stokes equations representing steady rotationally-symmetric flow, Quart. J. Mech.; Appl. Math. 5 (1951) 29–41.

[5] Owen J.M., Hayenes C.M., Bayley F.J., Heat transfer from an air-cooled rotating disk, Proc. Roy. Soc. London Ser. A 336 (1974) 453–473.

[6] Harmand S., Monnoyer F., Watel B., Desmet B., Echanges convectifs locaux sur une couronne d'un disque en rotation, Rev. Gén. Therm. 87 (1998) 885–897.

[7] Patra A.T., Pilichi C.D., Ferreira R.T.S., Local heat transfer in axially feeding radial flow beetween parallel disks, J. Heat Tran. 117 (1995) 47–53.

[8] Soong C.Y., Yan W.M., Numerical study of mixed convection between two corotating symmetrically heated discs, J. Thermophys. Heat Tran. 7 (1) (1993) 165–170.